

# The first detection of the solar U+III association with an antenna prototype for the future lunar observatory

L. A. Stanislavsky<sup>1</sup>, I. N. Bubnov<sup>1,2</sup>, A. A. Konovalenko<sup>1</sup>, P. L. Tokarsky<sup>1</sup> and S. N. Yerin<sup>1,2</sup>

<sup>1</sup> Institute of Radio Astronomy, Kharkiv, Ukraine; [lev.stanislavskiy@gmail.com](mailto:lev.stanislavskiy@gmail.com)

<sup>2</sup> V.N. Karazin Kharkiv National University, Kharkiv, Ukraine

Received 2020 December 11; accepted 2021 January 29

**Abstract** We report about observations of solar U+III bursts on 2020 June 5 by means of a new active antenna designed to receive radiation in 4–70 MHz. This instrument can serve as a prototype of the ultra-long-wavelength radio telescope for observations on the farside of the Moon. Our analysis of experimental data is based on simultaneous records obtained with the antenna arrays GURT and NDA in high frequency and time resolution, e-Callisto network as well as by using the space-based observatories STEREO and WIND. The results from this observational study confirm the model of Reid and Kontar.

**Key words:** Sun: corona — Sun: radio radiation — methods: data analysis — telescopes

## 1 INTRODUCTION

After a long break, the return of humans to the Moon has become extremely important for many reasons. On one hand, the Moon can serve as an ideal launching pad for building large-scale bases from which future space missions with direct human participation would begin to explore the other inner planets of our solar system, in particular Mars (Witze 2019; Dhingra 2018). On the other hand, the presence of a unique radio quiet zone on the lunar farside would allow observing very low-frequency emission from various cosmic objects almost not available for ground-based observations because of ionospheric cutoff as well as intensive artificial and/or terrestrial radio disturbances (Jester & Falcke 2009; Lazio et al. 2011; Mimoun et al. 2012; Zarka et al. 2012 and a recent link <https://www.space.com/nasa-telescope-far-side-of-moon.html>). The construction of a large scale radio array is not an easy task even on Earth, and on the other planets and moons this task is a major challenge for humanity to build scientific instruments in extreme conditions. The Ukrainian program of lunar explorations by spacecrafts has been suggested by Shkuratov et al. (2019), and perspective steps to solar studies with the help of radio observations on the lunar farside were considered by Stanislavsky et al. (2018). Advancing this program as applied to radio astronomy purposes, we produced an antenna prototype for the future lunar telescope at ultra-long wavelengths. It can record

radio emission of cosmic objects both independently and as parts of antenna arrays or interferometers. Its important advantage is a feasibility of preliminary approbation on Earth, receiving radio emission at frequencies close to ionospheric cutoff and higher. The present paper is just devoted to real observations as a test of this antenna demonstrating the scope of this instrument for exploring the Universe at ultra-long wavelengths in radio emission. Consequently, we observed and study the solar type U radio burst associated with type III bursts that are useful to examine possible models of the event.

## 2 INSTRUMENT

The great interest in the development of small-sized active dipoles for low-frequency radio astronomy has noticeably intensified theoretical and experimental studies of antenna technology, amplifiers and related components (see Konovalenko et al. 2016 and references therein). Over fifteen years of experience in operating active dipoles at the Giant Ukrainian Radio Telescope (GURT) ground-based radio array demonstrated their reliability and validity for scientific results. These dipoles, being small in size, provide optimal “radio astronomical sensitivity,” which is determined primarily by the contribution of the amplifier temperature to the noise temperature of the active dipole. In the case of a noise-free amplifier, the noise temperature of the active dipole is equal to the antenna temperature, obtained from observations of the Galactic background

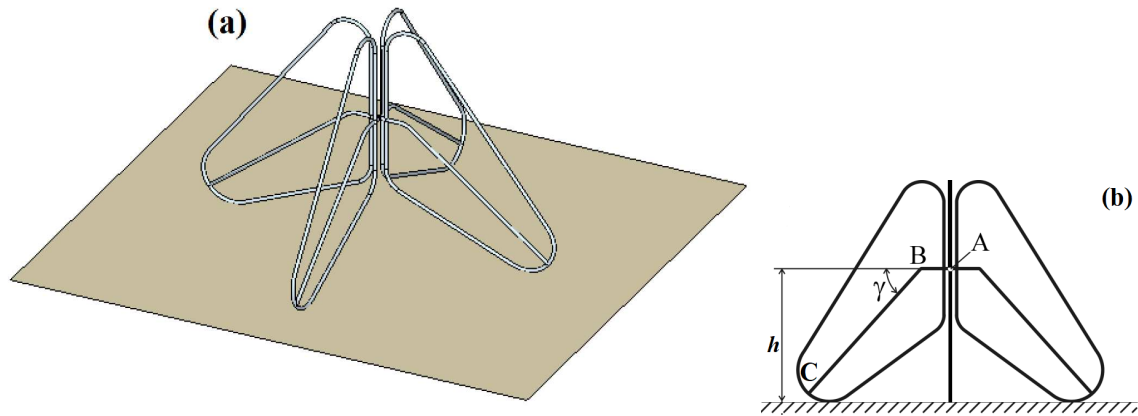


**Fig. 1** Sketch of the antenna prototype (a) with its frontal projection (b).

radio emission. A good result is considered to achieve the contribution of the amplifier temperature to the noise temperature of the active dipole no more than 10% – 25%. In this way, the corresponding studies were carried out to develop a prototype of the ultra-long-wavelength broadband antenna for radio astronomy purposes in which the Moon is an instrument location.

By numerical simulations of the antenna prototype and performing measurements of its parameters, we have studied the complex geometry of an active-dipole antenna, located above a partially conductive ground (Tokarsky et al. 2017). A sketch of this antenna is featured in Figure 1. Consequently, a computer model of this antenna was developed, which allowed us to obtain its characteristics (impedance, energy parameters, radiation pattern) in the operating frequency domain of 1 to 70 MHz. As a part of these studies, the dipole and amplifier were designed and manufactured as an active antenna, capable of receiving cosmic radiation in the frequency band 4–70 MHz. Test measurements of the Galactic background radiation were successfully conducted at the Radio Astronomical Observatory of S. Ya. Braude in terrestrial conditions. The antenna design was the following. The dipole arm lengths along the midline (ABC in the frontal projection of Fig. 1) are 2.8 m, the angle  $\gamma$  of inclination to the horizontal plane is  $45^\circ$  and the dipole terminals are located at  $h = 1.7$  m above ground. It is made of steel tubes having a diameter of 23 mm. As an antenna amplifier, the low-noise amplifier (LNA) with PHEMT transistors is used (Korolev 2014). The LNA nominal gain is  $G_{\text{amp}} = 22$  dB, the effective noise temperature is about 50 K and the 3rd order nonlinear distortion coefficient is more than  $30 \text{ dB } \mu\text{V}^{-1}$ . The LNA is supplied with a voltage of 5 V at the current consumption of 40 mA.

The spectrum records of solar radio emission were obtained by utilizing the receiver DSP-Z (an abbreviation for digital spectropolarimeters of type Z) which is a standard

**Table 1** Evolution of AR 12765 (see <https://www.spaceweatherlive.com/en/solar-activity/region/12765>)

Data	Number of sunspots	Size (MH)	Class Magn.	Location (deg)
2020/06/03	2	70	$\alpha$	S24E71
2020/06/04	2	100	$\alpha$	S24E58
2020/06/05	3	130	$\beta$	S24E44
2020/06/06	5	110	$\beta$	S22E33
2020/06/07	6	100	$\beta$	S23E20
2020/06/08	7	100	$\beta$	S24E07
2020/06/09	4	70	$\beta$	S24W06
2020/06/10	1	50	$\alpha$	S24W21
2020/06/11	1	50	$\alpha$	S22W35
2020/06/12	1	50	$\alpha$	S26W46
2020/06/13	1	60	$\alpha$	S25W60
2020/06/14	1	20	$\alpha$	S25W73
2020/06/15	1	10	$\alpha$	S26W86

device for the radio telescope UTR-2 (Zakharenko et al. 2016). This allows performing real-time Fast Fourier transform (FFT) analysis in two independent channels whose operating frequency band is 0–33 MHz. Since the prototype antenna can receive radio emission up to 70 MHz, we applied a special technique for records of radio emission in the frequency band twice as wide as the receiver can perform in each channel separately. While one channel received radio signals in the frequency range 4–33 MHz, another operated within 33–66 MHz. Their combination gave the spectrum of radio emission within 4–66 MHz. Based on the technique, the frequency and time resolutions were 4 kHz and 100 ms, respectively, in each channel.

### 3 OBSERVATIONS

Radio emission of solar bursts is often divided into types from the analysis of their observed frequency drift rate. The most numerous among the solar bursts are type III bursts (see, for example, Reid & Ratcliffe 2014 with references therein). They are caused by high velocity

electron beams accelerated by unstable magnetic fields in the solar atmosphere, and because of this, their frequency drift rate is extremely high. Typically, the type III bursts manifest a monotonic shape in dynamic spectra, going from high to low frequencies, showing the motion of beams to Earth. However, sometimes the closed magnetic fields on the Sun can change this exhibition in dynamic spectra. Their overall spectral signature resembles the letters J and U, and the bursts are therefore called type J and type U, respectively (Fokker 1970; Labrum & Stewart 1970; Stone & Fainberg 1971; Caroubalos et al. 1973; Morosan et al. 2017). It is generally accepted that the origin of these bursts is explained by the fact that the beam electrons travel along closed magnetic field lines, and therefore the frequency drift velocity is inverted (Zhelezniakov 1969). The motion of electrons from low to high density regions causes an increase of radio emission with frequency, whereas if the electron beam moves away from the Sun, the frequency of radio emission decreases (Leblanc et al. 1983; Aschwanden et al. 1992). The exciters, going through the corona, can produce simultaneous emission at the fundamental and the second harmonic of the local coronal plasma frequency. In comparison with ordinary type III bursts, both U and J bursts occur rarely. In our observations we detected a unique event in which the U burst was surrounded not only by type III bursts, but associated with some of them being interplanetary.

Although the Sun in the summer of 2020 was at solar activity minimum, nevertheless, activity still sometimes occurred. In particular, on 2020 May 29, the sunspot group caused the largest solar flare in a long period, starting from October 2017. This flare was M class, and it could be seen as the beginning of the awakening of the Sun after a long period of inactivity. Recall that the solar flare strength is denoted by letters A, B, C, M and X with decimal subclasses. The smallest of them is A-class, whereas X-class flares are the most intense. The M-class flare allowed us to assume continuation of solar activity in the following days and a chance for recording solar radio bursts in early June 2020. In fact, a new active area, namely NOAA AR 12765, appeared on the limb from the eastern side of the Sun on 2020 June 3 (see Table 1). At first it consisted of a single spot (<https://www.spaceweatherlive.com/en/solar-activity/region/12765>), which turned into a small bipolar region on 2020 June 5, close to the north-east of the initial spot position. Generally, sunspots can have different sizes and shapes. On this day the size of sunspots was the largest for this active region (AR). Its maximum value was 130 MH (in “millionths of the visible solar hemisphere”). It should be mentioned that most sunspot groups cover an area comparable to the

entire surface area of the Earth (which is almost 170 MH), but larger sunspot groups can easily reach 1000 MH or even much more (Meadows 2002). In the following days, the region remained in the  $\beta$  class, but decaying, after June 10 it moved to the  $\alpha$  class until it disappeared completely, going to the farside of the Sun. Note that the B6 (faint) flare occurred in this region at  $\sim 21:33$  UT on 2020 June 8.

Bipolar magnetic fields are interesting primarily because they can be responsible for type U solar radio bursts. It was such a burst that we managed to successfully record on 2020 June 5 (Fig. 2) with the help of the antenna prototype for future lunar radio telescopes. The change of sign in the frequency drift rate from negative to positive in this burst was clearly seen in the frequencies of  $\sim 20$  MHz to  $\sim 15$  MHz. Due to low solar activity, in general, the cutoff frequency of the Earth’s ionosphere at our latitude is noticeably lower than 10 MHz (on some days even reaching frequencies of 2 MHz). This makes it possible to conduct radio observations at frequencies pretty close to those that are planned to record with lunar observatories. Therefore, the received bursts were confidently detected at extremely low frequencies close to 6 MHz, despite numerous natural and artificial radio interferences. A much more detailed spectrum above 8 MHz was provided by recording this event with the GURT antenna array (Fig. 3). This active antenna consists of 25 cross-dipoles, five in each row and column. Dipole arms have east-west and north-south orientations. The instrument serves for receiving radio emission within 8–80 MHz (Konvalenko et al. 2016). As the sensitivity of the GURT array is higher than that of one dipole antenna, its dynamic spectrum represents many (less intense) type III solar bursts that are clearly visible before the solar U burst. Moreover, the latter has a fine structure.

Space-based observations with the STEREO A and WIND spacecrafts at this time support our detection ([https://solar-radio.gsfc.nasa.gov/data/WWaves-SWAVES/2020/wind\\_stereo\\_20200605.pdf](https://solar-radio.gsfc.nasa.gov/data/WWaves-SWAVES/2020/wind_stereo_20200605.pdf)). Unfortunately, the highest frequencies of these radio instruments ( $\sim 16$  MHz and  $\sim 13.8$  MHz, respectively) did not allow noticing all the details of this event. Nevertheless, the observations show continuation of the solar radio event up to 100 kHz which may be interpreted as an interplanetary type III burst (Fig. 4). Interestingly, this result manifests an important feature of this event. We observe the separation of electron beams into two parts. One part, due to the deflection of beams by solar magnetic fields back to the Sun, caused the emergence of the U-shaped burst, whereas another followed in the opposite direction to Earth, producing traces on the dynamic spectra, characteristic of solar bursts of type III, merging together. The types of solar bursts,

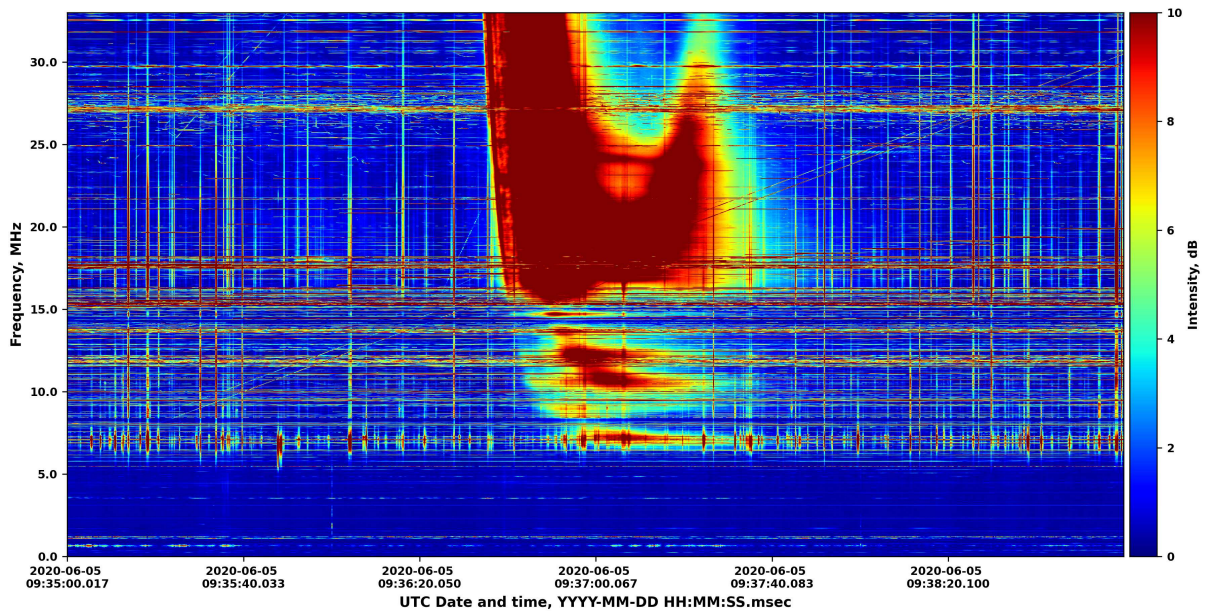


**Fig. 2** Dynamic spectrum of the solar U+III bursts (observed on 2020 June 5) with the help of an antenna prototype intended for ultra-long-wavelength records. The prominent narrow vertical and horizontal lines indicate numerous intensive radio disturbances generated by natural lightning discharges and broadcast stations, respectively.

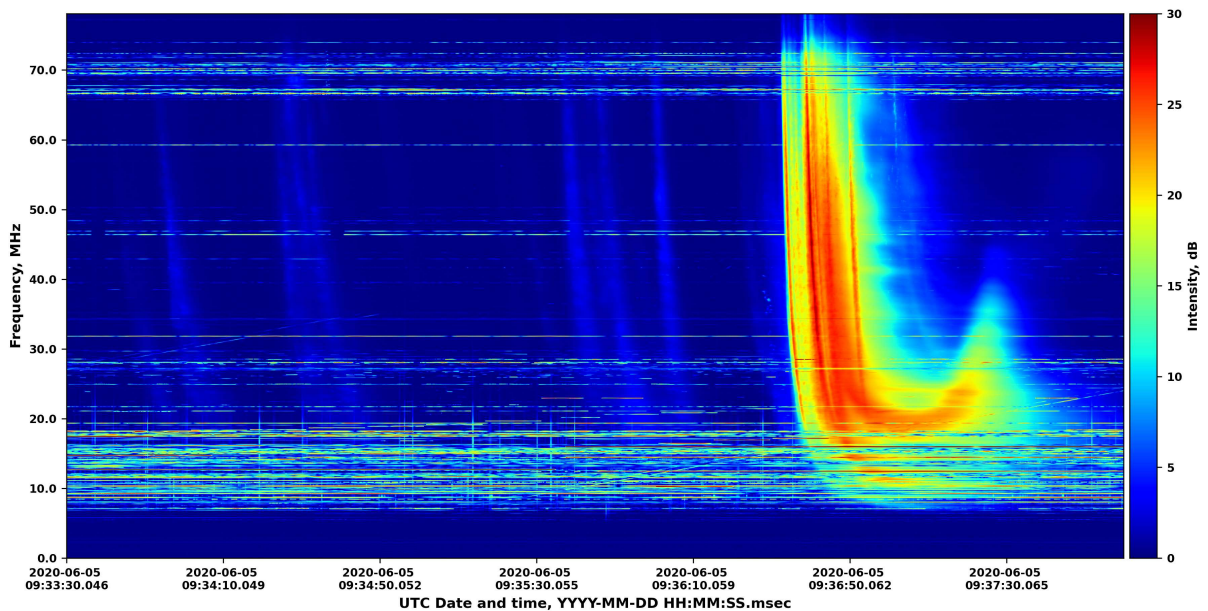


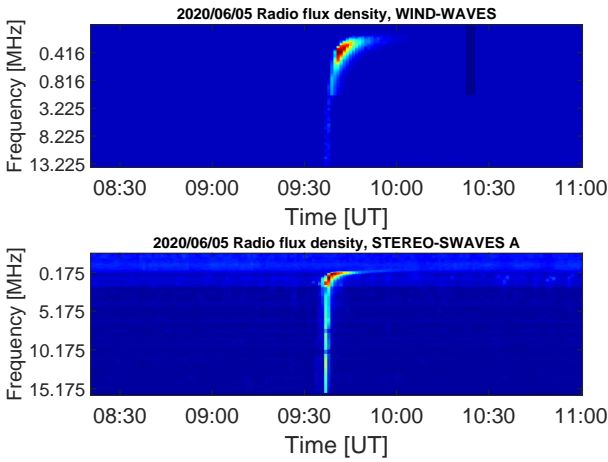
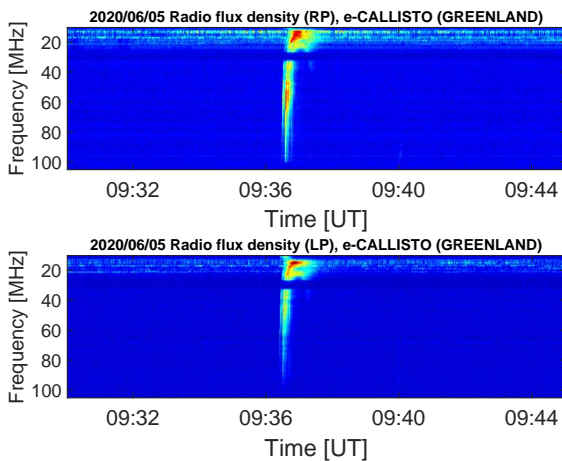
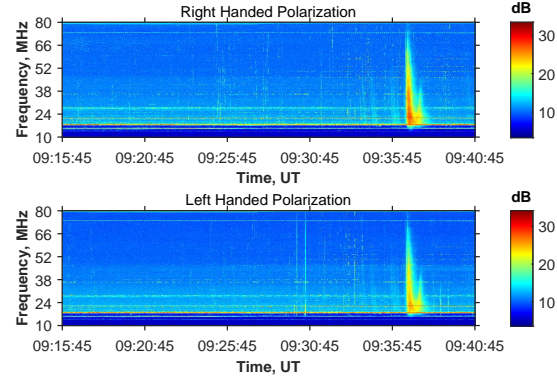
**Fig. 3** Dynamic spectrum of many solar bursts at  $\sim 09:37$  UT on 2020 June 5 obtained with the active antenna array GURT (time resolution 100 ms, frequency resolution 38 kHz).

observed simultaneously, may be called U+III bursts, since they were connected with the same place (AR 12765) on the Sun and generated by the same group of associated electron beams. The U+III event is superimposed on a series of weaker type III bursts.

To confirm this concept, we have found the U-shaped burst in the observations made on other suitable radio telescopes, which had a similar low-frequency range for recording solar radio emission. One of the e-Callisto network stations (Benz et al. 2009), located in Greenland

**Table 2** High frequency cutoff for the U+III bursts, observed on 2020 June 5 at  $\sim$ 09:37 UT, from the e-Callisto network data (see <http://soleil.i4ds.ch/solarradio/callistoQuicklooks/?date=20200605>).

Country	Location	Frequency range (MHz)	Cutoff (MHz)
Denmark	Copenhagen, DTU	45–100	85
United Kingdom	Glasgow, UOG	45–81	> 81
Switzerland	Landschlacht, HB9SCT	15–85	82
Switzerland	Landschlacht, HB9SCT	45–155	84
Switzerland	Heiterswil, Kant	45–81	> 81
Austria	Michelbach, Lensch	20–90	75
Belgium	Humain, ROB	45–435	80–90
India	Bangalore, GAURI	45–410	85
Denmark	Kangerlussuaq, Greenland	10–95	85–90

**Fig. 4** Dynamic spectra of radio emission recorded with the solar space-based observatories WIND and STEREO A on 2020 June 5, according to <https://solar-radio.gsfc.nasa.gov/data/wind/rad2> and [https://solar-radio.gsfc.nasa.gov/data/stereo/new\\_summary](https://solar-radio.gsfc.nasa.gov/data/stereo/new_summary).**Fig. 5** Dynamic spectra of radio emission in right (RP) and left (LP) handed polarizations from the solar observations on 2020 June 5 with the e-Callisto network station in Greenland. In the upper part of the spectra, the track similar to a type III burst can be seen, separated from the type U burst branch with a negative frequency drift rate.**Fig. 6** Dynamic spectra of solar radio emission on 2020 June 5 observed with NDA in Nançay.

(ISR Kellyville observatory near Kangerlussuaq,  $66^{\circ} 59' 8.88''$  N,  $50^{\circ} 56' 44.26''$  W), recorded the solar U-shaped burst at the same time that we did (see Table 2). Let us mention a little about hardware features of this station for solar observations: the frequency domain of 10 to 95 MHz is divided into 200 frequency channels each of which has the band of 475 kHz, and the time resolution is 250 ms. The antenna consists of one broadband low-frequency antenna intended for the Long Wavelength Array (LWA, see <http://lwa.phys.unm.edu>). The spectra obtained by the e-Callisto station (see Fig. 5) are morphologically identical to the spectrum obtained by our instruments, which had noticeably both better sensitivity and higher frequency-time resolution. There is no doubt that the records show the same event, manifesting the solar U-shaped burst. Moreover, fragments of this event were also detected with other e-Callisto stations. It is also worth mentioning that this group of solar bursts was recorded by the Nançay Decametric Array (NDA) in France. The dynamic spectrum is displayed in Figure 6. The radio telescope provides daily observations of solar radio emission at 10–80 MHz. Its  $2 \times 72$  helical spiral antennas are for polarization measurements (Boischot et al. 1980), and the solar NDA data are freely available for viewing (via the link <https://realtime.obs-nancay>).

$f_r$ ). Using the variety of radio astronomy tools in our comparison, we conclude that the observed U+III bursts have a solar origin and cannot be associated with ionospheric disturbances and/or equipment malfunctions.

#### 4 RESULTS

According to Reid & Kontar (2017), the generation of radio emission in the form of the solar U bursts simultaneously with type III bursts requires strictly defined conditions. Initially, having a negative velocity gradient, an injected electron beam cannot generate radio emission because of its stable distribution function with respect to Langmuir wave production. Nevertheless, when it propagates through the solar corona, a positive velocity gradient becomes its feature, making the beam unstable and producing a solar burst. The propagation effects determine a starting height with which the burst is nascent. The value is  $0.6 R_\odot$  (from the solar photosphere). Although it is dependent on parameters of beams, its value may be taken as an estimate. If one assumes that this conjecture is true, with its help we can calibrate the electron density model of the solar corona (see more details below). Before  $0.6 R_\odot$ , an electron beam does not produce radio emission, but after that three regimes are possible. The electron beam with too low a density still does not emit. In the second regime, for moderate densities, a beam travels along open magnetic field lines, producing only type III bursts. The third regime, the most interesting for us, is characterized by high initial electron beam densities, that is good for generating both type III and type U bursts in radio emission. In this case the magnetic loop should be large enough for propagation effects, making the electron beam unstable, until it reaches the loop top and turns back to the Sun. This does not exclude the generation of type III bursts, due to the movement of beams along open magnetic field lines. As a rule, radio emission of type U bursts has a weaker and more diffuse shape for the positive frequency drift rate branch (Aurass & Klein 1997). The fine structure of the U+III bursts manifests many radio sources tracing a similar path through the corona so that each of the radio patterns was produced by its electron beam.

Using the Newkirk (one-fold) model for the solar corona (Newkirk 1961), the radial change in the electron density is written as

$$n_e(r) = \alpha \cdot 4.2 \cdot 10^4 \cdot 10^{(4.32/r)}, \quad (1)$$

where  $n_e(r)$  is the electron density of coronal plasma in  $\text{cm}^{-3}$ , depending on the heliocentric height  $r$  in solar radii. This  $\alpha$ -fold model describes the electron density profile well above quiet equatorial regions ( $\alpha = 1$ ), in dense loops ( $\alpha = 4$ ) and in extremely dense loops for  $\alpha = 10$  (Koutchmy 1994; Mann et al. 2018), but the value of the parameter  $\alpha$

is indicative. As the local plasma frequency  $f_{pe}$  (in MHz) equals

$$f_{pe} = 8.9 \cdot 10^{-3} \sqrt{n_e}, \quad (2)$$

then the source height and the radiation frequency are linked by a simple expression

$$r = \frac{2.16}{\lg f - 0.26 - 0.5 \lg \alpha}, \quad (3)$$

where  $f$  is the radiation frequency in MHz. As applied to our event and following Table 2, the U+III bursts started with  $\sim 85$  MHz that corresponds to the heliocentric height  $\sim 1.6 R_\odot$  (or  $\sim 0.6 R_\odot$  from photosphere) under  $\alpha \approx 4$ . This is in good agreement with conjectures of Reid & Kontar (2017). Note that the high-frequency cutoff finding allows calibrating the value of  $\alpha$  for the coronal density model. The top of the U burst reached  $\sim 15$  MHz, i.e., the height was about  $3.5 R_\odot$ , taking  $\alpha \approx 4$ . At the pivot point the instantaneous bandwidth was about 5 MHz, permitting us to estimate the loop width at the top. It was about  $0.6 R_\odot$ . Recall that the activity on solar regions depends of their size (Solanki 2003). The larger it is, the higher the probability of occurrence of flares, coronal mass ejections, diversity of solar bursts and their intensity. AR 12765 developed from the unipolar form to bipolar, and we observed the only U burst, when the size of this region was maximum. Thus, one can assume that each bipolar AR with the size of more than 110 MH will be able to generate electron beams with high initial densities, resulting in radio emission of the U bursts simultaneously and together with type III bursts. Finally, it should be noticed that according to Figure 3 and Figure 6, the U+III bursts are surrounded by weaker type III bursts which were caused by electron beams with moderate densities. This case can correspond to the second regime mentioned above.

#### 5 CONCLUSIONS

Having such an extensive set of radio and optical observations on 2020 June 5, we can confidently assert that the event at  $\sim 09:37$  UT included the solar U burst combined with type III bursts. Evidently, they were generated by many electron beams accelerated in AR 12765 and traveling in the solar corona along both closed and open magnetic field lines. The uniqueness of this phenomenon lies in the fact that magnetic fields in AR 12765 only developed between a unipolar ( $\alpha$  class) and a bipolar configuration ( $\beta$  class). This was due to low solar activity. The configuration of magnetic fields and the size of the AR were favorable to the emergence of solar bursts of such types. Observations with help of various radio instruments allowed us to explore this event in more detail and to get reliable results, confirming the model of this phenomenon. Moreover, this research also gave a number

of new interesting footings related to the development of ultra-long-wavelength antennas for future lunar radio telescopes.

**Acknowledgements** The authors thank the WIND, STEREO, NDA and e-Callisto network teams for their instrument maintenance and open data access. This research was partially supported by Research Grant (0120U101334), and authors acknowledge the National Academy of Sciences of Ukraine for this support. The authors are also thankful to Dorovskyy V.V. for helpful discussions.

## References

- Aschwanden, M. J., Bastian, T. S., Benz, A. O., & Brosius, J. W. 1992, *ApJ*, 391, 380
- Aurass, H., & Klein, K. L. 1997, *A&AS*, 123, 279
- Benz, A. O., Monstein, C., Meyer, H., et al. 2009, *Earth Moon and Planets*, 104, 277
- Boischot, A., Rosolen, C., Aubier, M. G., et al. 1980, *Icarus*, 43, 399
- Caroubalos, C., Couturier, P., & Prokaxis, T. 1973, *A&A*, 23, 131
- Dhingra, D. 2018, *Geosciences*, 8, 498
- Fokker, A. D. 1970, *Sol. Phys.*, 11, 92
- Jester, S., & Falcke, H. 2009, *New Astron. Rev.*, 53, 1
- Konovalenko, A., Sodin, L., Zakharenko, V., et al. 2016, *Experimental Astronomy*, 42, 11
- Korolev, A. M. 2014, *Russian Radio Physics and Radio Astronomy*, 19, 181 (in Russian)
- Koutchmy, S. 1994, *Advances in Space Research*, 14, 29
- Labrum, N. R., & Stewart, R. T. 1970, *Proceedings of the Astronomical Society of Australia*, 1, 316
- Lazio, T. J. W., MacDowall, R. J., Burns, J. O., et al. 2011, *Advances in Space Research*, 48, 1942
- Leblanc, Y., Poquerusse, M., & Aubier, M. G. 1983, *A&A*, 123, 307
- Mann, G., Breitling, F., Vocks, C., et al. 2018, *A&A*, 611, A57
- Meadows, P. 2002, *Journal of the British Astronomical Association*, 112, 353
- Mimoun, D., Wiczcerek, M. A., Alkalai, L., et al. 2012, *Experimental Astronomy*, 33, 529
- Morosan, D. E., Gallagher, P. T., Fallows, R. A., et al. 2017, *A&A*, 606, A81
- Newkirk, Gordon, J. 1961, *ApJ*, 133, 983
- Reid, H. A. S., & Kontar, E. P. 2017, *A&A*, 606, A141
- Reid, H. A. S., & Ratcliffe, H. 2014, *RAA (Research in Astronomy and Astrophysics)*, 14, 773
- Shkuratov, Y. G., Konovalenko, A. A., Zakharenko, V. V., et al. 2019, *Acta Astronautica*, 154, 214
- Solanki, S. K. 2003, *A&A Rev.*, 11, 153
- Stanislavsky, A. A., Konovalenko, A. A., Yerin, S. N., et al. 2018, *Astronomische Nachrichten*, 339, 559
- Stone, R. G., & Fainberg, J. 1971, *Sol. Phys.*, 20, 106
- Tokarsky, P. L., Konovalenko, A. A., & Yerin, S. N. 2017, *IEEE Transactions on Antennas and Propagation*, 65, 4636
- Witze, A. 2019, *Nature*, 571, 153
- Zakharenko, V., Konovalenko, A., Zarka, P., et al. 2016, *Journal of Astronomical Instrumentation*, 5, 1641010
- Zarka, P., Bougeret, J. L., Briand, C., et al. 2012, *Planet. Space Sci.*, 74, 156
- Zhelezniakov, V. V. 1969, *Radio Emission of the Sun and Planets* (Oxford, New York, Pergamon Press)